ChemCatChem

Perspective
doi.org/10.1002/cctc.202400567

Chemistry Europe
European Chemical Societies Publishing

www.chemcatchem.org

How to Break the Activity-Stability Conundrum in Oxygen Evolution Electrocatalysis: Mechanistic Insights

Tobias Binninger,*[a] Genevieve C. Moss,[b] Ziba S. H. S. Rajan,[b] Rhiyaad Mohamed,[b] and Michael H. Eikerling[a, c]

Technically viable electrocatalysts for the oxygen evolution reaction (OER) must be both active and stable under the harsh conditions at an electrolyser anode. While numerous highly active metal-oxide catalysts have been identified, only very few are sufficiently stable, with iridium oxides being the most prominent. In this perspective, we draw insights from OER mechanisms to circumvent the activity-stability conundrum generally plaguing the development of OER catalysts. In the commonly considered OER mechanisms, one or several metal-oxygen (M–O) bonds are required to be broken along the OER pathway, providing a mechanistic link between the OER and oxide decomposition. However, a recently discovered mechanism on crystalline iridium dioxide provides a new OER pathway without M–O bond breakages, thus enabling the combination of sufficient activity and stability.

Introduction

Efficiently catalyzing the oxygen evolution reaction (OER) remains a key challenge for the commercialization of water electrolysis technologies at scale. The demanding kinetics of the OER require the use of rare catalyst materials based on platinum-group-metals (PGMs), such as iridium and ruthenium. At strongly acidic or alkaline pH and anode potentials exceeding 1.5 V_{RHE}, catalyst corrosion is a severe issue. Under these conditions, all metals, including noble metals, are oxidized and in principle, only metal oxides can therefore be stable. However, even most metal oxide catalysts were observed to undergo corrosion during OER.[1–4] In this respect, crystalline, rutile iridium dioxide (IrO_2) is a rather unique case, offering the combination of both high OER activity and good stability, and therefore is the state-of-the-art anode catalyst in commercial proton-exchange-membrane water electrolysers (PEMWEs). Owing to the scarcity of iridium, however, it is necessary to substantially reduce iridium loadings at electrolyser anodes, or strive towards the use of more earth-abundant materials, to enable large-scale deployment of PEMWE technology.[5] The development of affordable OER electrocatalysts which are both highly active and stable is thus a key challenge in electrocatalysis research for water electrolysis. While major efforts have focused on the search for materials with better activity, the importance of addressing the issue of long-term stability has become widely recognized more recently.[6,7] Improvements in catalyst stability are not only required for efficient long-term operation of electrolysers, but also for enabling further crucial reductions in catalyst loadings.

Contextualizing recent contributions, in this perspective we discuss the mechanistic relationship between OER activity and catalyst (in)stability. We first review the often-observed correlation between OER activity and catalyst corrosion from thermodynamic and kinetic perspectives. Subsequently, the exceptional case of crystalline IrO_2 and its consequences for design strategies towards stable OER catalysts are discussed. This perspective focuses on the acidic OER, while catalyst corrosion is less of a problem under alkaline conditions. It should be noted, however, that the key principles of the thermodynamic coupling between OER and catalyst instability, as well as the proposed mechanistic descriptors for the respective decoupling essentially apply to both acidic and alkaline conditions.

[a] *Dr. T. Binninger, Prof. Dr. M. H. Eikerling*
Theory and Computation of Energy Materials (IEK-13), Institute of Energy and Climate Research, Forschungszentrum Jülich GmbH,
52425 Jülich, Germany
E-mail: t.binninger@fz-juelich.de

[b] *G. C. Moss, Z. S. H. S. Rajan, Dr. R. Mohamed*
HySA/Catalysis Centre of Competence, Catalysis Institute, Department of Chemical Engineering, University of Cape Town, 7701, South Africa

[c] *Prof. Dr. M. H. Eikerling*
Chair of Theory and Computation of Energy Materials, Faculty of Georesources and Materials Engineering, RWTH Aachen University, Intzestrasse 5, 52072 Aachen, Germany

Thermodynamic Coupling Between the OER and Catalyst Instability

Experimental evidence for a coupling between the OER and catalyst corrosion has been presented for a variety of metal-oxide catalysts.[1–4] This seemingly universal phenomenon has led some of us to prove that *any* metal oxide becomes thermodynamically unstable under OER conditions.[8] While the processes of OER and oxide corrosion might not appear related at a first glance, a fundamental link was revealed in the form of the so-called lattice oxygen evolution reaction (LOER). To illustrate this, we consider the OER,

$$2\,OH^- \rightleftarrows \frac{1}{2}\,O_2 + H_2O + 2\,e^-, \quad (1)$$

written here under alkaline conditions. Due to the autoprotolysis equilibrium of water, $OH^- + H^+ \rightleftarrows H_2O$, the same thermodynamic treatment remains valid for the OER under acidic conditions, $H_2O \rightleftarrows \frac{1}{2}O_2 + 2\,H^+ + 2\,e^-$. Metal-oxide corrosion often involves dissolution into the electrolyte,

$$MO_n + n\,H_2O \rightleftarrows M^{2n+} + 2n\,OH^-, \quad (2)$$

where M^{2n+} refers to the dissolved metal cation. For the sake of clarity, this process is written as a chemical reaction with an unchanged valency of the cation. Often, however, dissolution involves changes in cation valency, which can be treated along the same lines albeit including electrochemical electron transfer. The LOER process reads:[8]

$$MO_n \rightleftarrows M^{2n+} + \frac{n}{2}\,O_2 + 2n\,e^-. \quad (3)$$

It corresponds to the oxidation of oxygen anions from the metal-oxide lattice to form molecular oxygen, accompanied by the dissolution of metal cations into the electrolyte. As visualized in Figure 1, the three processes of OER (1), dissolution (2), and LOER (3) are coupled, i.e., any one of them can be written as a sequence of the other two. Therefore, if two of the three processes are at equilibrium, the third is automatically also at equilibrium. On the contrary, if the OER is driven out of equilibrium, it follows by *reductio ad absurdum* that at least one of the other two processes must also depart from equilibrium.

Under OER conditions, the thermodynamic driving force points from left to right in Eq. (1) (top to bottom along the right-hand edge in Figure 1). Depending on the concentration of dissolved metal cations, $c_{M^{2n+}}$, three scenarios are distinguished.[8]

(i) If the concentration is less than the saturation concentration for dissolution, $c_{M^{2n+}} < c^{sat}_{M^{2n+}}$, the metal oxide is thermodynamically unstable due to the simple dissolution process (2).

(ii) If the concentration is equal to the saturation concentration, $c_{M^{2n+}} = c^{sat}_{M^{2n+}}$, the dissolution process (2) is at equilibrium and the LOER must experience the same driving force as the OER (top to bottom along the left-hand edge in Figure 1).

(iii) As a consequence of (ii), the LOER process would result in a local oversaturation of the electrolyte, $c_{M^{2n+}} > c^{sat}_{M^{2n+}}$, and trigger redeposition on the metal oxide surface in the reverse direction of Eq. (2) (right to left along the top edge in Figure 1).

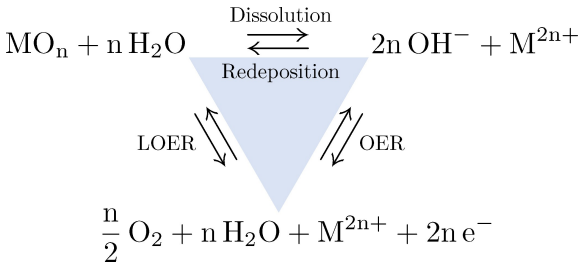

Figure 1. The reactions of LOER, OER, and dissolution stand in a triangular relationship – any one of them can be written as a sequence of the other two.

It should be emphasized that these considerations concern the *thermodynamic* coupling of OER and catalyst instability, which does not necessarily imply coupling of the respective kinetics.[9] The kinetic/mechanistic perspective will be discussed later on. The established universal thermodynamic instability of oxides under OER conditions does not contradict the thermodynamic stability of certain metal oxides suggested by Pourbaix analyses. To resolve the apparent contradiction, it must be noted that Pourbaix diagrams are constructed from a defined set of possible corrosion reactions under the assumption that the metal/oxide/water system is equilibrated at a given applied potential, E (and solution pH). Reactions involving the gas phase, however, such as the OER and LOER, cannot be accounted for in a Pourbaix diagram, because the respective equilibria would require the oxygen pressure, p_{O_2}, to satisfy the Nernst equation,

$$E = E^{\ominus}_{OER} + \ln(10)\,\frac{RT}{4F}\,\log_{10}\left(\frac{p_{O_2}}{p^{\ominus}_{O_2}}\right), \quad (4)$$

with $E^{\ominus}_{OER} = 1.23\,V_{RHE}$ the equilibrium potential at $p^{\ominus}_{O_2} = 1$ bar standard pressure. At typical OER potentials, *i.e.*, $E > 1.5\,V_{RHE}$, Eq. (4) yields an equilibrium pressure of the order of 10^{18} bar, which is clearly beyond any physically realistic situation. However, this demonstrates that (i) enormous oxygen pressures would be required to stabilize the metal oxide at OER potentials and (ii) Pourbaix diagrams, strictly speaking, do not apply to out-of-equilibrium OER conditions at ambient, or near ambient, oxygen pressures.

Dynamic Stability and Self-Healing: The Dissolution-Redeposition Cycle

According to the thermodynamic arguments discussed in the previous section, the system can reach a quasi-steady state according to scenario (iii), where the LOER drives a dissolution-redeposition cycle (DRC) of metal cations.[8] Employing *operando* X-ray absorption spectroscopy, Fabbri et al.[4] observed structural transformation of a Ba–Sr–Co–Fe (BSCF) perovskite into Fe–Co oxide under OER conditions. This could be explained with a DRC driving dissolution of metal cations, whereby highly soluble Ba and Sr cations are lost to the bulk electrolyte while less soluble Fe and Co cations are redeposited onto the oxide surface. Chung et al.[10] performed inductively coupled plasma mass spectrometry (ICP-MS) measurements with isotope-labelled Fe–Ni/Co oxides to show that Fe surface sites were dynamically stable in a DRC after adding small amounts of dissolved Fe ions to the electrolyte. This is closely related to the

concept of self-healing, or self-repair, introduced by Nocera et al.[11,12] for cobalt-P_i catalysts prepared by self-assembly from aqueous solutions of Co^{2+} and phosphate (P_i). This concept has also been demonstrated for manganese oxide catalyst under acidic conditions.[13] Self-repair by redeposition of dissolved cations can thus provide dynamic stability to intrinsically unstable OER catalysts. While this appears to be a viable approach for electrolysis technologies based on liquid electrolytes, the required presence of dissolved cation species is problematic for polymer-electrolyte technologies, such as PEMWEs and anion-exchange-membrane water electrolysers (AEMWEs).

Mechanistic Coupling Between the OER and Catalyst Instability

Having discussed the thermodynamic perspective, the question arises about the relationship between OER and catalyst instability in terms of reaction kinetics and the mechanism involved. Decoupling the kinetics of OER and LOER could, in principle, render a metal oxide sufficiently (meta)stable for the envisaged operation time of an electrolyser. The following discussion is based on three commonly considered OER mechanisms: the classical adsorbate evolution mechanism (AEM),[14] the binuclear peroxo mechanism (BPM),[15–17] and the lattice oxygen mechanism (LOM).[18] We note that different nomenclatures are used for these mechanisms, sometimes implying subtle differences in certain reaction steps. The BPM has also been referred to as 'oxide path mechanism' (OPM),[7,19] but we prefer the term BPM to better distinguish it from the LOM. We will first review the essential differences between these mechanisms before discussing their relationship to catalyst (in)stability.

The classical AEM is commonly written as a sequence of four electron-proton removal steps that proceed via the surface-adsorbed intermediates OH, O, and OOH,[14]

$$M^* + H_2O \rightarrow M{-}OH + H^+ + e^- \quad (5)$$

$$M{-}OH \rightarrow M{-}O + H^+ + e^- \quad (6)$$

$$M{-}O + H_2O \rightarrow M{-}OOH + H^+ + e^- \quad (7)$$

$$M{-}OOH \rightarrow M^* + O_2 + H^+ + e^- \quad (8)$$

where M* denotes a free adsorption site on top of a coordinately unsaturated surface metal cation. It has been pointed out that the final step must be considered as two sequential elementary steps,[20,21]

$$M{-}OOH \rightarrow M{-}OO + H^+ + e^- \quad (9)$$

$$M{-}OO \rightarrow M^* + O_2 \quad (10)$$

with a deprotonation of OOH to form an adsorbed OO and subsequent desorption to release a free O_2 molecule.

The BPM (also known as OPM)[7,19] was frequently considered for molecular oxygen-evolving complexes,[15–17] but also metal oxide catalysts.[20,22,23] As a main difference to the AEM, the oxygen molecule is formed *via* association of two neighboring on top oxygen atoms,

$$M{-}O + M{-}O \rightarrow 2M^* + O_2 \quad (11)$$

which results in the formation of two unsaturated metal cations. It must be noted that most computational studies have treated this step simultaneous with re-adsorption of one or two H_2O (or OH^-) molecules.[7,16] As recently pointed out by some of us, this approach should be taken with care, because it can hide the actual energetic barrier by ignoring the unsaturated state of surface cations.[21]

The LOM has been proposed by Rong et al. for certain perovskite-type catalysts.[18] Similar to the BPM, the oxygen-oxygen (O–O) bond is formed *via* internal coupling. However, in the case of the LOM, only one of the involved species is a top-adsorbed surface oxygen, while the other is a bridge oxygen (M–O–M) from the surface layer of the oxide lattice,

$$M{-}O{-}M + M{-}OH \rightarrow M^*V_O{}^*M + M{-}OO + H^+ + e^- \quad (12)$$

The O_2 molecule is subsequently released in a desorption step (10). The O–O coupling step (12) results in the formation of an oxygen vacancy (V_O) in the surface oxide layer, which requires breaking of two metal-oxygen (M–O) bonds. The LOM can therefore only proceed on oxides with a weak lattice bond strength and, thus, low bulk stability.[18] The catalytic cycle is closed by insertion and deprotonation of H_2O (or OH^-) at the vacancy site,

$$M^*V_O{}^*M + H_2O \rightarrow M{-}O{-}M + 2H^+ + 2e^- \quad (13)$$

However, if the rate of this step is not entirely balanced with step (12), more and more oxygen vacancies will accumulate in the surface oxide layer, destabilizing the metal cations and triggering dissolution into the electrolyte. The LOM thus establishes a close mechanistic link between OER and LOER. Comparing the LOM and AEM pathways on a series of perovskite catalysts, Rong et al.[18] found increasing OER activity and a switching from AEM to LOM with decreasing bulk stability.

The number of metal-oxygen bonds split along a given OER pathway, N^{split}_{M-O}, represents an intuitive descriptor for the kinetic coupling of OER activity and metal oxide instability. Figure 2 depicts the critical M–O bond breaking steps for the different mechanisms. The LOM requires breaking of two lattice bonds (M–O–M) in step (12) and one surface M–O bond in the final desorption step (10). This is only feasible for oxides with poor stability. The AEM, on the other hand, requires breaking of only one surface M–O bond to release the O_2 molecule from the top adsorption site, *cf.* steps (10) or (8). Finally, two surface M–O bonds get broken in step (11) for the BPM, which thus falls in

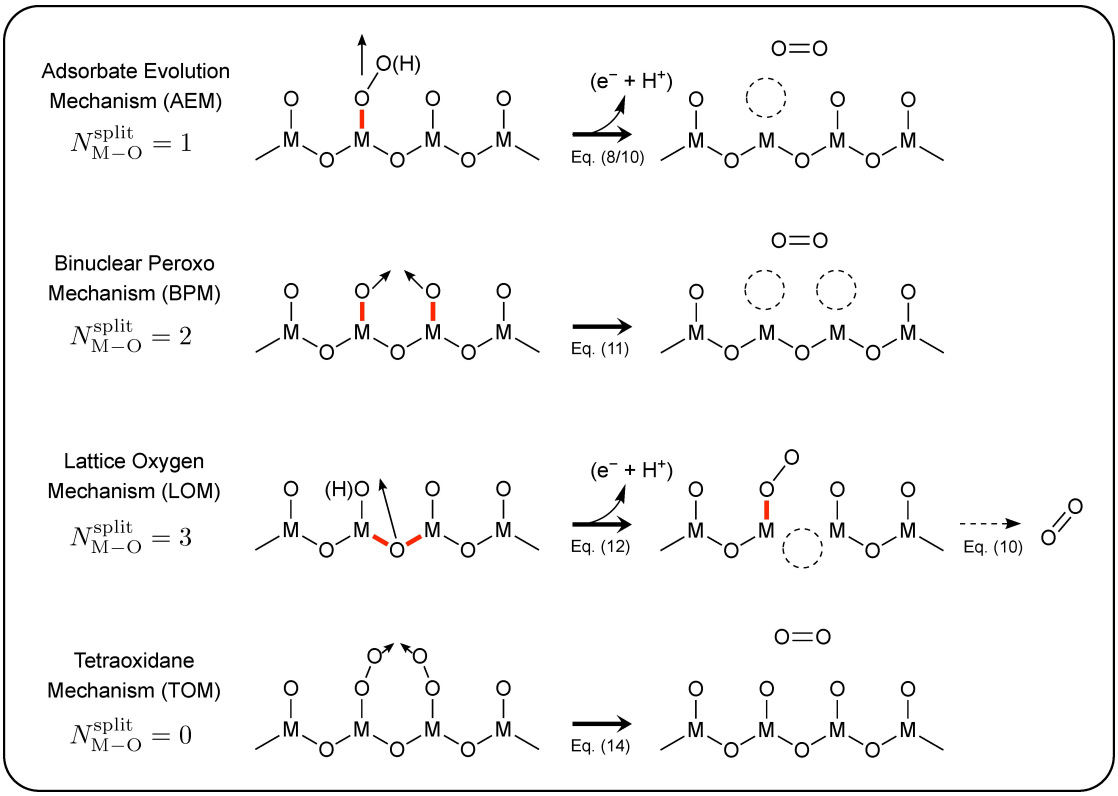

Figure 2. Critical steps of the AEM, BPM, and LOM involving the breakage of metal-oxygen bonds (highlighted in red). The number of bond breakages along a given pathway, $N^{\text{split}}_{\text{M-O}}$, indicates to what degree the kinetics of the OER and oxide decomposition are coupled. The TOM mechanism does not involve any M–O bond breakages.

between the LOM and AEM. Out of these mechanisms, the AEM would thus be expected to enable the best combination of OER activity and catalyst stability. However, at least one surface metal-oxygen bond must be split in all of the commonly considered mechanisms. According to the Sabatier principle, the respective bond strength must neither be too strong nor too weak for achieving optimal OER activity. On the other hand, maximum strength of metal-oxygen bonds in the oxide lattice is required for optimal bulk stability. The similar nature of lattice and surface M–O bonds thus imposes a trade-off in the optimisation towards activity *vs.* stability.

A Novel Mechanism for Combining Activity and Stability

A general correlation between OER activity and oxide instability thus derives from both thermodynamic and kinetic perspectives. Crystalline iridium dioxide, however, represents a prominent exception to this rule, displaying both high activity and stability. This was clearly demonstrated by Over et al.,[24,25] who observed perfect stability of single-crystalline IrO_2 (110) films even at anodic potentials of 2.1 V_{SHE} and concluded that "single-crystalline IrO_2 (110) films are much more stable than hitherto expected".[24] The origin of the superior performance of crystalline iridium dioxide was recently explained by Binninger and Doublet,[26] who revisited the classical mechanism of the OER at the IrO_2 (110) surface. A very high energy barrier of about 0.9 eV was found for the final step (10), suggesting the desorption of the O_2 molecule to be inhibited by the strength of the Ir–OO bond. Most previous studies have only considered the respective free energy change, which is significantly lowered by final-state gas-phase entropy contributions, and therefore overlooked the critical role of the desorption step.[21]

While the suggested strength of the Ir–O bond explains the remarkable stability of crystalline iridium dioxide, the material would be expected to be a poor OER catalyst due to over-binding of the reaction product, in disagreement with the experimentally established excellent activity of IrO_2. To resolve this contradiction, Binninger and Doublet proposed a new pathway bypassing the critical desorption step and avoiding the breaking of an Ir–O bond. The evolving O_2 molecule is formed by association of two neighboring M–OO entities,

$$\text{M}{-}\text{OO} + \text{M}{-}\text{OO} \rightarrow 2\,\text{M}{-}\text{O} + \text{O}_2, \tag{14}$$

passing through a M–OOOO–M transition state.[26] We note that this pathway was also proposed by Curutchet et al. as a competing alternative to the AEM on CoOOH,[27] who recognized the similarity between the O_4 intermediate and the tetraoxidane molecule (H_2O_4).[28] We therefore refer to the pathway involving step (14) as 'tetraoxidane mechanism' (TOM). Since no metal-oxygen bonds are broken, the TOM kinetically

decouples the OER from LOER/oxide decomposition. It can proceed on metal oxides with high M–O bond strength and enables excellent OER activity of IrO_2.[26]

As an alternative to the TOM, Exner[29] recently proposed that the M–O bond breaking in step (10) of the AEM could be facilitated by simultaneous bond formation due to adsorption of a water molecule in a step similar to the Walden inversion. Indeed, Walden inversion steps have been shown to be involved in the dissolution mechanism of tetrahedrally coordinated RuO_4 entities at a reconstructed RuO_2(100) surface by Hess and Over.[30] However, in most oxide catalysts for the OER, metal cations have an octahedral coordination environment that provides little space for attack by Walden inversion and can sterically protect the metal cation. This is supported by the study of Ping et al.[20] who performed simulations of the concomitant O_2 desorption and H_2O adsorption at the IrO_2 (110) surface. It was found that desorption and adsorption proceed one after the other. The feasibility of concerted breaking and re-formation of M–O bonds at the catalyst surface thus depends on the coordination environment of surface cations and must be evaluated by explicit barrier calculations.[21]

Implications

The new understanding of the origin for combined activity and stability of IrO_2 has implications for the design of material-efficient, high-performing catalysts for the OER. Firstly, the exceptional role of crystalline iridium dioxide is highlighted, encouraging the development of novel synthesis routes towards nano-crystalline IrO_2 with maximum active surface area and high degree of crystallinity.[6,31] At the same time, however, the question arises why amorphous iridium oxides (IrO_x) are much less stable and more prone to dissolution than their crystalline counterparts.[3] It will have to be clarified whether this is due to the nature of iridium-oxygen bonds present in IrO_x, possibly related to the increased presence of Ir^{3+} species,[32] or whether amorphous IrO_x presents iridium species that are sterically accessible for attack by Walden inversion.[29,30] Additional studies on the mechanistic coupling between the OER and dissolution of iridium oxides are therefore needed.[33–35] Last but not least, we believe that these mechanistic insights have relevance for the development of strategies towards accelerated catalyst discovery. Besides evaluating the free energies of relevant OER intermediates, computational studies for catalyst screening should explicitly account for the O_2 desorption step (10) of the AEM as well as the O_4 association step (14) of the TOM. A high energy barrier of the former and a low barrier of the latter, together with a high coverage of the M–OO intermediate, would indicate interesting candidate materials for combined performance in both OER activity and stability.

In summary, the activity-instability relationship in OER electrocatalysis has been explained from both a thermodynamic and mechanistic perspective and routes to circumvent this conundrum have been highlighted. The commonly considered AEM, BPM, and LOM mechanisms require the breaking of different numbers of metal-oxygen bonds, thus kinetically coupling the processes of OER and catalyst decomposition. In contrast, no metal-oxygen bonds are split along the TOM pathway, which therefore kinetically decouples activity from oxide instability. We hope that this perspective can give new stimulus to the development of cost-effective and high-performing OER catalysts.

Acknowledgements

The presented work was carried out within the framework of the Helmholtz Association's program Materials and Technologies for the Energy Transition under the topic Chemical Energy Carriers and the subtopic Electrochemistry for Hydrogen. G.C.M., Z.S.H.S.R., and R.M. would like to thank the Department of Science and Innovation (DSI), for providing funding through the Hydrogen South Africa (HySA) Catalysis Centre of Competence Programme. Open Access funding enabled and organized by Projekt DEAL.

Conflict of Interests

There are no competing interests to declare.

Data Availability Statement

Data sharing is not applicable to this article as no new data were created or analyzed in this study.

Keywords: Oxygen Evolution Reaction (OER) · Lattice Oxygen Evolution Reaction (LOER) · OER Mechanism · Activity-Stability Trade-off · Iridium oxide (IrO_2)

[1] K. J. May, C. E. Carlton, K. A. Stoerzinger, M. Risch, J. Suntivich, Y.-L. Lee, A. Grimaud, Y. Shao-Horn, *J. Phys. Chem. Lett.* **2012**, *3*, 3264.
[2] N. Danilovic, R. Subbaraman, K.-C. Chang, S. H. Chang, Y. J. Kang, J. Snyder, A. P. Paulikas, D. Strmcnik, Y.-T. Kim, D. Myers, V. R. Stamenkovic, N. M. Markovic, *J. Phys. Chem. Lett.* **2014**, *5*, 2474.
[3] S. Cherevko, T. Reier, A. R. Zeradjanin, Z. Pawolek, P. Strasser, K. J. J. Mayrhofer, *Electrochem. Commun.* **2014**, *48*, 81.
[4] E. Fabbri, M. Nachtegaal, T. Binninger, X. Cheng, B.-J. Kim, J. Durst, F. Bozza, T. Graule, R. Schäublin, L. Wiles, M. Pertoso, N. Danilovic, K. E. Ayers, T. J. Schmidt, *Nat. Mater.* **2017**, *16*, 925.
[5] C. Minke, M. Suermann, B. Bensmann, R. Hanke-Rauschenbach, *Int. J. Hydrogen Energy* **2021**, *46*, 23581.
[6] H. Dhawan, M. Secanell, N. Semagina, *Johnson Matthey Technology Review* **2021**, *65*, 247.
[7] C. Rong, K. Dastafkan, Y. Wang, C. Zhao, *Adv. Mater.* **2023**, *35*, 2211884.
[8] T. Binninger, R. Mohamed, K. Waltar, E. Fabbri, P. Levecque, R. Kötz, T. J. Schmidt, *Sci. Rep.* **2015**, *5*, 12167.
[9] K. S. Exner, *ChemCatChem* **2021**, *13*, 4066.
[10] D. Y. Chung, P. P. Lopes, P. Farinazzo Bergamo Dias Martins, H. He, T. Kawaguchi, P. Zapol, H. You, D. Tripkovic, D. Strmcnik, Y. Zhu, S. Seifert, S. Lee, V. R. Stamenkovic, N. M. Markovic, *Nat. Energy* **2020**, *5*, 222.
[11] M. W. Kanan, D. G. Nocera, *Science* **2008**, *321*, 1072.
[12] D. A. Lutterman, Y. Surendranath, D. G. Nocera, *J. Am. Chem. Soc.* **2009**, *131*, 3838.
[13] M. Huynh, D. K. Bediako, D. G. Nocera, *J. Am. Chem. Soc.* **2014**, *136*, 6002.
[14] J. Rossmeisl, Z. W. Qu, H. Zhu, G. J. Kroes, J. K. Nørskov, *J. Electroanal. Chem.* **2007**, *607*, 83.

[15] U. Bossek, T. Weyhermueller, K. Wieghardt, B. Nuber, J. Weiss, *J. Am. Chem. Soc.* **1990**, *112*, 6387.
[16] M. Busch, E. Ahlberg, I. Panas, *Phys. Chem. Chem. Phys.* **2011**, *13*, 15069.
[17] M. Busch, E. Ahlberg, I. Panas, *J. Phys. Chem. C* **2013**, *117*, 288.
[18] X. Rong, J. Parolin, A. M. Kolpak, *ACS Catal.* **2016**, *6*, 1153.
[19] T. Reier, H. N. Nong, D. Teschner, R. Schlögl, P. Strasser, *Adv. Energy Mater.* **2017**, *7*, 1601275.
[20] Y. Ping, R. J. Nielsen, W. A. I. Goddard, *J. Am. Chem. Soc.* **2017**, *139*, 149.
[21] T. Binninger, P. M. Kowalski, M. H. Eikerling, *Curr. Opin. Electrochem.* **2023**, *42*, 101382.
[22] G. Lodi, E. Sivieri, A. De Battisti, S. Trasatti, *J. Appl. Electrochem.* **1978**, *8*, 135.
[23] K. Macounova, M. Makarova, P. Krtil, *Electrochem. Commun.* **2009**, *11*, 1865.
[24] T. Weber, V. Vonk, D. Escalera-López, G. Abbondanza, A. Larsson, V. Koller, M. J. Abb, Z. Hegedüs, T. Bäcker, U. Lienert, G. S. Harlow, A. Stierle, S. Cherevko, E. Lundgren, H. Over, *ACS Catal.* **2021**, *11*, 12651.
[25] H. Over, *ACS Catal.* **2021**, *11*, 8848.
[26] T. Binninger, M.-L. Doublet, *Energy Environ. Sci.* **2022**, *15*, 2519.
[27] A. Curutchet, P. Colinet, C. Michel, S. N. Steinmann, T. L. Bahers, *Phys. Chem. Chem. Phys.* **2020**, *22*, 7031.
[28] D. J. Mckay, J. S. Wright, *J. Am. Chem. Soc.* **1998**, *120*, 1003.
[29] K. S. Exner, *Adv. Sci.* **2023**, *10*, 2305505.
[30] F. Hess, H. Over, *ACS Catal.* **2023**, *13*, 3433.
[31] M. Malinovic, P. Paciok, E. S. Koh, M. Geuß, J. Choi, P. Pfeifer, J. P. Hofmann, D. Göhl, M. Heggen, S. Cherevko, M. Ledendecker, *Adv. Energy Mater.* **2023**, *13*, 2301450.
[32] V. Pfeifer, T. E. Jones, J. J. V. Vélez, C. Massué, M. T. Greiner, R. Arrigo, D. Teschner, F. Girgsdies, M. Scherzer, J. Allan, M. Hashagen, G. Weinberg, S. Piccinin, M. Hävecker, A. Knop-Gericke, R. Schlögl, *Phys. Chem. Chem. Phys.* **2016**, *18*, 2292.
[33] O. Kasian, J.-P. Grote, S. Geiger, S. Cherevko, K. J. J. Mayrhofer, *Angew. Chem. Int. Ed.* **2018**, *57*, 2488.
[34] A. Zagalskaya, V. Alexandrov, *J. Phys. Chem. Lett.* **2020**, *11*, 2695.
[35] F. Hess, *Curr. Opin. Electrochem.* **2023**, *41*, 101349.

Manuscript received: March 24, 2024
Revised manuscript received: April 26, 2024
Version of record online: June 12, 2024